APPLICATION OF MOLECULAR CONNECTIVITY AND ELECTRO-TOPOLOGICAL INDICES IN QUANTITATIVE STRUCTURE ACTIVITY ANALYSIS OF PYRAZOLE DERIVATIVES AS INHIBITORS OF FACTOR XA AND THROMBIN

Chandravel Krishnasamy,[#] *Arjun Raghuraman,*[#] *Lemont B. Kier*[$] *and Umesh R. Desai*[*,#$]

[#]Department of Medicinal Chemistry, [#]Institute for Structural Biology and Drug Discovery, and [$]Center for the Study of Biological Complexity, Virginia Commonwealth University, Richmond, VA

Running Title: QSAR of Factor Xa and Thrombin Inhibition

Keywords: QSAR; molecular connectivity; E-state; structure-activity relationships; factor Xa; thrombin; inhibition; pyrazoles;

[*] Address correspondence to this author at the Institute for Structural Biology and Drug Discovery, 800 East Leigh Street, Suite 212, Richmond, VA 23219. Ph. (804)828-7328; Fax (804)827-3664; E-mail: urdesai@vcu.edu

Prepared for *Chemistry and Biodiversity*

Abstract

Factor Xa and thrombin, two critical pro-coagulant enzymes of the clotting cascade, are the primary target of current anticoagulation research that aims to develop potent, orally bioavailable, synthetic small molecule inhibitors. To determine structural features that might play important roles in factor Xa and thrombin recognition and oral bioavailability, quantitative structure-activity and structure-property analysis was performed on the factor Xa and thrombin inhibition data and Caco-2 cell permeability data of 3-substituted pyrazole 5-carboxamides reported by Pinto et al. [J. Med. Chem. 44 (2001) 566]. The factor Xa and thrombin inhibition potencies and Caco-2 cell permeability of the 3-substituted pyrazole 5-carboxamides could be quantitatively described through molecular connectivity and atom level E-state indices. Different quantitative structure-activity and structure-property models were derived for each of the three biological properties. The models are statistically relevant with correlation co-efficients of at least 0.9 and contain only 2 or 3 molecular descriptor variables. The study demonstrates the use of molecular connectivity and E-state indices in understanding factor Xa and thrombin inhibition. In addition, the models may be useful for predictive purposes in generating molecules with better potency, specificity and oral bioavailability.

1. Introduction

Factor Xa and thrombin are two serine proteases that play a pivotal role in the blood coagulation cascade [1-5]. Factor Xa represents the confluence of the intrinsic and extrinsic pathways of the cascade and activates prothrombin to thrombin. Thrombin has several pro-coagulant functions including the activation of platelets, the feedback activation of several other coagulation factors, and the conversion of fibrinogen to insoluble fibrin clots. Inhibition of thrombin results in a near complete disruption of clot formation and hence, numerous thrombin inhibitors have been vigorously investigated as anticoagulants [6-10]. However, growing realization that inhibiting the proteolytic function of thrombin results in numerous ancillary effects has led to an impetus to design selective factor Xa inhibitors. It is expected that molecules specifically inhibiting factor Xa are less likely to inhibit platelet function resulting in less bleeding complications.

Numerous scaffolds have been investigated as inhibitors of factor Xa [11-25]. A majority of these scaffolds utilize the presence of an amidine group, an Arg mimic, to target the enzyme's active site. Yet, this group may also recognize thrombin and other Arg specific proteases resulting in considerable loss of inhibition specificity. Thus, the design of factor Xa specific inhibitors has to rely on structural features of the scaffold to induce selective recognition of the factor Xa active site. To understand whether such structural features can be identified, we analyzed the quantitative structure – activity relationships (QSAR) in a series of 3-substituted pyrazole 5-carboxamides that were reported to inhibit factor Xa and thrombin [23]. Our QSAR study reveals that three biological end points, factor Xa and thrombin inhibition potency and Caco-2 cell permeability may be quantitatively described using molecular connectivity and atom level electro-topological state indices. The study suggests that it should be possible to utilize the

molecular connectivity and E-state indices-based models, in combination with combinatorial library prepared using different substituents, for the design of useful leads that enhance the factor Xa potency and specificity, and oral bioavailability.

2. Experimental

2.1 Data set

The data used in this study was taken from the literature published by Pinto et al. [23], wherein the synthesis and screening of several small molecules for direct inhibition of thrombin and factor Xa is reported. Although the synthesized compounds were screened against both human and rabbit factor Xa, only the human enzyme data is considered for this QSAR study. Both the factor Xa and thrombin inhibitory activity were expressed as equilibrium inhibition constants (K_I, nM), which are averaged from multiple determinations. The pyrazole scaffold was found to be the most potent scaffold and hence, to work with a homogenous data set we performed our QSAR study on these compounds only. Within this set, the compounds with indeterminate K_I values were excluded from the study. Both the factor Xa and thrombin inhibition constants were converted to the pK_I values, where pK_I = –logK_I, for use as dependent variables.

In addition to factor Xa and thrombin inhibition potencies, Pinto et al. [23] also report the Caco-2 cell permeability screening of selected pyrazole derivatives. Caco-2 cell permeability assay [26] is an in vitro technique to gain preliminary knowledge about the oral bioavailability of potential drugs. Cell permeability is reported as apparent permeability (P_{APP}, cm/s). The oral bioavailability potential corresponds directly to the P_{APP} value. The reported P_{APP} values for the limited number of pyrazole derivatives were converted to the pP_{APP} values, where pP_{APP} = –log P_{APP}, for QSAR analysis.

2.2 Molecular modeling and descriptor calculation

The chemical structures of pyrazole derivatives were prepared using **ISIS** v2.5 software (Elsevier MDL, San Ramon, CA) and exported as mol files to calculate their structural descriptor values. Kier and Hall have developed simple, yet structurally informative descriptors, such as the electro-topological state (E-state) indices, molecular connectivity indices and kappa shape indices [27-29] to explore the relationship between structure and activity.

The E-State is derived as a composite index embracing both electronic and steric attributes of atoms in molecules. As reported in a number of studies, the E-State is a unified property of an atom that reflects its own electronegativity and that of the proximal and distal atoms, as well as its topological state [28]. In contrast to the E-state index, the molecular connectivity indices transform a molecular structure into different mathematical models. More specifically, the structural information is compiled into a single number utilizing a specific mathematical model that represents the number and type of bonds as well as the pattern of bonding. Multiple such mathematical models can be derived from different bonding pattern representations of a single molecular structure giving several molecular connectivity indices. Kappa shape indices are topological indices that encode a molecule's shape in one of many forms such as the degree of cyclicity, the spatial density of atoms in the molecule, or the degree of centrality of branching. Several authors have exploited the power of these structural descriptors in the quantitative analysis of physical, chemical, biological and toxicological properties [30-38].

Structural descriptors used in our QSAR study were calculated using **QSARIS** software v2.1 (Elsevier MDL, San Ramon, CA). This program incorporates an automated search of more than 100 electronic, thermodynamic, structural and topological molecular descriptors that may be

important for understanding the activity parameter. For QSAR analysis of factor Xa and thrombin inhibition data as well as for Caco-2 cell permeability data, we used a genetic algorithm (GA), as reported previously [39,40]. Briefly, the GA was initialized with 32 chromosomes selected at random from the entire set of molecular descriptors. These chromosomes were transformed using Friedman's lack-of-fit fitness function and subject to the tournament selection procedure to select parents for crossover. A crossover rate of 0.5 was used and the offspring was subject to a mutation rate of 0.1. The algorithm was run for 2000 generations, which typically gave a stable model and no improvement was noted beyond this point.

3. Results

3.1 QSAR analysis of factor Xa inhibition

QSAR analysis of inhibition of factor Xa by pyrazole derivatives was performed using QSARIS program that utilizes a genetic algorithm-based approach to fit the observed data to a multi-parameter regressional model. The data could be readily fitted to several models containing five or six molecular descriptors, each giving an r^2 value of 0.94 or more. However, to arrive at a statistically relevant QSAR model, we restricted the number of molecular descriptors to $\sqrt{n} - 2$, where n is the total number of compounds in the data set. Thus, the maximum number of allowed molecular descriptors was set to 3. However, when the GA was performed with only three molecular descriptor variables, the algorithm did not converge reproducibly suggesting in no solution corresponding to a significant QSAR model. It is likely that the presence of a large number of molecular descriptors greatly increased the search space resulting in inadequate search. To address this likelihood, the GA was performed using an enhanced mutation rate, which rapidly converged to a unique solution.

In an alternative study, the genetic algorithm was initialized using a subset of molecular descriptors. In other words, the entire set of molecular descriptors was divided into smaller subsets and the GA was run within each subset. The smaller subsets were generated in a non-exclusive manner so that several subsets had overlapping molecular descriptors. This resulted in several models that repeatedly contained a small number of molecular descriptors. This approach identified the group of molecular descriptors that were enriched, which were further confirmed in an independent study.

Both the global search and the alternative compiled subset search resulted in a unique QSAR solution (Model 1) containing three descriptors.

$$-\log K_{I_{(fXa)}} = 1.32\ SHssNH + 1.67\ {}^{3}\chi_c^{v} + SdssC\_acnt + 1.75 \qquad \textbf{[Model 1]}$$

$r^2 = 0.902$, $s = 0.329$, $q^2 = 0.408$, $n = 26$

where *SHssNH* is the atom-type hydrogen E-state for sp^3 hybridized NH nitrogen, *SdssC_acnt* is the count of non-aromatic sp^2 hybridized carbons, ${}^{3}\chi^{v}_{c}$ is the third-order valence connectivity cluster index, and $K_{I(fXa)}$ is the equilibrium factor Xa inhibition constant.

The presence of *SHssNH* in the model indicates that the hydrogen atom of the amide bond (Figure 1) plays an important role in the binding of the pyrazole derivatives, perhaps through the formation of a hydrogen bond. *SdssC_acnt*, which is a count of certain type of carbons, does not provide any information regarding the nature of binding, however, it is a powerful identifier of potency-enhancing functional groups because it can assume distinct values, either 1 (benzylamine) or 2 (benzamidine). The presence of this molecular descriptor in model 1 captures the experimental result that the benzamidine analogs are more potent than the benzylamine analogs (Table 1). Finally, ${}^{3}\chi^{v}_{c}$ is a non-empirical index that encodes information on the constitutive property of a molecule, e.g., the degree of branching, the branching pattern, the

degree of cyclicity [27]. It is difficult to transcribe the value of this index into discrete structural component(s), however it has been loosely interpreted as a measure of intermolecular accessibility [41].

We reasoned that it should be possible to replace *SdssC_acnt* with a molecular descriptor that captures the 'functional group identification' feature but, in addition, can also provide information on the substitution pattern. Hence, we decided to test *SHdNH*, the atom-type E-state index for the imine group (Figure 1). This index would assume a value of zero for all benzylamine analogs but is likely to be sensitive to substitutions at the 3-position of the pyrazole for benzamidine derivatives. Using this E-state index, model 2 was obtained.

$$-\log K_{I(fXa)} = 1.33\ SHssNH + 1.68\ {}^{3}\chi_c^{v} + 0.23\ SHdNH + 3.500 \qquad \textbf{[Model 2]}$$

$r^2 = 0.901$, s = 0.330, $q^2 = 0.369$, n=26

Models 1 and 2 describe the variation in factor Xa inhibition potency equally well as judged by the r^2 value. Interestingly, molecular descriptors *SHssNH* and ${}^{3}\chi^{v}_{c}$, present in model 1, are also found to play important role in model 2. Finally, all three molecular descriptors have positive co-efficients suggesting the value of these parameters and factor Xa inhibition potency are positively correlated.

3.2 Structural Interpretation of the factor Xa QSAR analysis

To better understand the importance of these descriptors, we assessed the variation in factor Xa inhibition potency as a function of the substitution pattern at the R_1, R_2, R_3, R_4 and X positions on the pyrazole scaffold (Table 2). Four pyrazole analogs, **2a**, **2b**, **2c** and **14a**, display factor Xa inhibition constants ($K_{I(fXa)}$) in the range of 13 to 160 pM arising from functional group variation at the R_1 position (Figure 1). Calculation of the values of the E-state (*SHssNH* and *SdNH*) and molecular connectivity (${}^{3}\chi^{v}_{c}$) descriptors for this sub-set of pyrazole derivatives

indicates that only $^{3}\chi^{v}_{c}$ parallels changes in the $K_{I(fXa)}$ values (Table 2). This suggests that any substitution at the R_1 position that increases the value of $^{3}\chi^{v}_{c}$ parameter is likely to enhance the factor Xa inhibition potency.

The R_2 position assumes only two substitutions, either $–CH_2NH_2$ or $–C(NH)NH_2$, which have been analyzed above through the E-state descriptor, *SdNH*. A comparison of pyrazoles **17a** and **2b** further confirms this observation (Table 2) and shows that the other two descriptors, *SHssNH* and *χvc3*, are not positively correlated with $K_{I(fXa)}$.

Comparison of pyrazoles **2h**, **2g**, **2f**, **2b** and **2c** shows that the factor Xa inhibition potency decreases from 8 pM to 1300 pM. In this sub-set, replacing the –H group with the –F,–CF_3, $–SO_2NH_2$, and $–SO_2CH_3$ substituents increases the K_I value ~3-, 30-, 100- and 160-fold, respectively (Table 2). Calculation of the values for the three molecular descriptors suggests that only ($^{3}\chi^{v}_{c}$) values parallel the observed change in $K_{I(fXa)}$ suggesting that the extent of connectivity and valence state of the groups at the R_3 position appear to play an important role in factor Xa inhibitory activity. Likewise, the large variation in the *SHssNH* value suggests that the R_4 position cannot tolerate a $–CH_3$ group, as can be noted from a comparison of pyrazoles **2d** and **2b** (Table 2).

Despite the apparently good structural correlation noted above, a word of caution is necessary. The molecular descriptors identified by QSAR models 1 and 2 do not fully explain the change in $K_{I(fXa)}$ value of pyrazoles **2b**, **2i**, **2k**, **2m** and **2l**, each of which exhibit only one change in the substituent at the X-position (Table 2). In this sub-set of pyrazole derivatives, the –CH group is replaced with electronegative substituents –N, –CF, –CCl and –CBr resulting minimal changes in the E-state indices, *SHssNH* and *SdNH*, but significant changes in molecular connectivity index $^{3}\chi^{v}_{c}$. Yet, the factor Xa inhibition potency of these molecules is nearly

identical (5 – 13 pM) (Table 2). This suggests that additional factors such as conformational transitions and protonation – deprotonation equilibrim (pK_A), which were not modeled at all in this exercise, may be important. Thus, QSAR models 1 and 2 are not exhaustive and should be implicated conservatively.

3.3 QSAR analysis of specificity of pyrazoles for inhibition of factor Xa

Although both factor Xa and thrombin bind molecules that contain arginine-mimicking groups [42,43], the presence of certain structural features in the organic inhibitors affords significant specificity of inhibition. In the case of 3-substituted pyrazole 5-carboxamides, the specificity of inhibition is strongly in favor of factor Xa (Table 1). A majority of pyrazole derivatives prefer to inhibit factor Xa nearly 5,000-fold better than thrombin, while the range of specificity was found to be 462–200,000-fold. To determine which structural features in the pyrazole derivatives determine the factor Xa inhibition specificity, we explored the use of molecular descriptors in a QSAR analysis of thrombin inhibition. Following an approach similar to that described above for factor Xa inhibition study, we obtained a statistically significant model 3 for thrombin inhibition.

$$-\log K_{I(Thr)} = 0.77\ SHdNH + 0.19\ {}^{2}\chi - 0.16\ SaaN + 2.63 \qquad \textbf{[Model 3]}$$

$$r^2 = 0.953,\ s = 0.193,\ q^2 = 0.933,\ n = 28$$

where *SHdNH* is the atom-type hydrogen E-state for imine nitrogens, ${}^{2}\chi$ is the second-order valence connectivity cluster index, and *SaaN* is the atom-type E-state for aromatic nitrogens.

Several interesting points can be inferred from the thrombin QSAR model 3. First, the correlation matrix (Table 4) indicates that none of the molecular descriptors, except for the two related descriptors (*SHdNH* and *SdaaC_acnt*, see above and Table 4 footnote) in the thrombin

model inter-correlate with the factor Xa model, either 1 or 2. Second, the E-state *SHssNH* index, which figures prominently in both factor Xa models, is not featured in thrombin inhibition model 3, suggesting that substituents that are able to enhance the hydrogen bond donor capability of the amide nitrogen (position X) should enhance the factor Xa inhibition specificity. Third, whereas ${}^{3}\chi^{v}_{c}$ is important for anti-factor Xa activity, a different connectivity index ${}^{2}\chi$ is important for direct thrombin inhibition. This suggests that the molecular features that recognize thrombin, outside of the amidine group in pyrazole derivatives, are significantly different from those important for factor Xa recognition. Finally, the negative co-efficient of the *SaaN* index, which corresponds to the electro-topological state of the aromatic nitrogen, suggests that compounds in the data set that contain pyridine or pyrimidine rings decrease binding affinity for thrombin.

3.4 QSAR analysis of Caco-2 cell permeability property of 3-substituted pyrazoles

To assess the oral bioavailability of the pyrazole class of inhibitors, Pinto et al. [23] report the Caco-2 cell permeability of nine derivatives of the 3-substituted pyrazole scaffold. Caco-2 cell permeability assay [26] has been routinely used as an in vitro technique to assess the oral bioavailability potential of small molecules. To determine whether factors that govern factor Xa potency and specificity contribute to oral bioavailability, we performed QSPR analysis using all the molecular descriptors studied above. QSPR analysis using the pP_{APP} values of nine pyrazole compounds suggests model 4 as the best description of their Caco-2 cell permeability.

$$-\log P_{APP} = 0.41\ SdssC - 3.51\ {}^{4}\chi^{v}_{p} + 21.84 \qquad \textbf{[Model 4]}$$

$r^2 = 0.9497$, s = 0.1515, $q^2 = 0.8907$, n =9

where *SdssC* is the atom-type hydrogen E-state for non-aromatic sp^2 hybridized carbons and ${}^{4}\chi^{v}_{p}$ is the fourth-order path connectivity cluster index.

The correlation matrix for model 4 (not shown) suggests that the major determinant of cell permeability is the fourth-order path connectivity index, $^4\chi^v_p$. This highlights the role of molecular surface in determining the Caco-2 cell permeability in this series of molecules. Thus, substituents that cause an increase in the $^4\chi^v_p$ value are predicted to increase the Caco-2 cell permeability. Likewise, the implication of hydrogen E-state for non-aromatic sp^2 hybridized carbons suggests that planar molecules, but containing fewer aromatic rings, are likely to enhance the oral bioavailability in the pyrazoles. Finally, the Caco-2 cell permeability model does not contain molecular descriptor terms that govern factor Xa (and thrombin) inhibition potency. Although this result may imply that factors governing inhibition and oral bioavailability are likely to be distinct, it is important to remember that molecular connectivity indices – $^2\chi$, $^3\chi^c_v$, and $^4\chi^v_p$ – are derived on the basis of connectivity present in the entire molecule and, hence, contain some overlapping characteristics.

4. Conclusions

The study of quantitative structure-activity and structure-property relationships revealed that factor Xa inhibition potency, specificity in inhibition of factor Xa and Caco-2 cell permeability of 3-substituted pyrazole 5-carboxamide derivatives can be successfully described using molecular connectivity indices and atom level E-state indices. An E-state index of the amide hydrogen, *SHssNH*, was found to play an important role in determining the affinity of these molecules, perhaps through hydrogen bonding. The models also suggest that substituents capable of enhancing the hydrogen bond donor property of the amide nitrogen are expected to enhance the specificity of factor Xa inhibition. The QSAR models implicate two different molecular connectivity indices, $^3\chi^v_c$ and $^2\chi$, for direct anti-factor Xa and anti-thrombin activity, respectively. Likewise, another molecular connectivity index, $^4\chi^v_p$, was found to be a good

predictor of Caco-2 cell permeability in a limited series of pyrazole derivatives. A mathematical analysis of E-state and molecular connectivity descriptors identified in this study for a combinatorial library prepared using different substituents on the pyrazole scaffold can be expected to provide useful leads on enhancing factor Xa potency and specificity, as well as improve potential oral bioavailability.

Acknowledgements

This work was supported by the National Heart, Lung and Blood Institute (RO1 HL069975 and R41 HL081972), the American Heart Association National Center (EIA 0640053N) and the A. D. Williams Foundation.

References

[1] U. R. Desai, Med. Res. Rev. 24 (2004) 151-181.

[2] J. P. Vacca, Annu. Rep. Med. Chem. 33 (1996) 81-90.

[3] R. D. Rosenberg, P. S. Damus, J. Biol. Chem. 248 (1973) 6498-6505.

[4] E. W. Davre, K. Fujikawa, W. Kisiel, Biochemistry 30 (1991) 10363-10370.

[5] J. S. Rosenberg, D. S. Beeler, R. D. Rosenberg, J. Biol. Chem. 250 (1995) 1607-1617.

[6] K. J. Stauffer, P. D. Williams, H. G. Selnick, P. G. Nantermet, C. L. Newton, C. F. Homnick, M. M. Zrada, S. D. Lewis, B. J. Lucas, J. A. Krueger, B. L. Pietrak, E. A. Lyle, R. Singh, C. B. Miller-Stein, R. B. White, B. Wong, A. A. Wallace, G. R. Sitko, J. J. Cook, M. A. Holahan, M. Stranieri-Michener, Y. M. Leonard, J. J. Lynch, Jr., D. R. McMasters, Y. Yan, J. Med. Chem. 48 (2005) 2282 – 2293.

[7] J. W. Nilsson, I. Kvarnström, D. Musil, I. Nilsson, B. Samulesson, J. Med. Chem. 46 (2003) 3985 – 4001.

[8] K. Lee, C. W. Park, W-H. Jung, H. D. Park, S. H. Lee, K. H. Chung, S. K. Park, O. H. Kwon, M. Kang, D-H. Park, S. K. Lee, E. E. Kim, S. K. Yoon, A. Kim, J. Med. Chem. 46 (2003) 3612 – 3622.

[9] C. S. Burgey, K. A. Robinson, T. A. Lyle, P. E. J. Sanderson, S. D. Lewis, B. J. Lucas, J. A. Krueger, R. Singh, C. Miller-Stein, R. B. White, B. Wong, E. A. Lyle, P. D. Williams, C. A. Coburn, B. D. Dorsey, J. C. Barrow, M. T. Stranieri, M. A. Holahan, G. R. Sitko, J.

J. Cook, D. R. McMasters, C. M. McDonough, W. M. Sanders, A. A. Wallace, F. C. Clayton, D. Bohn, Y. M. Leonard, T. J. Detwiler Jr., J. J. Lynch, Jr., Y. Yan, Z. Chen, L. Kuo, S. J. Gardell, J. A. Shafer, J. P. Vacca, J. Med. Chem. 46 (2003) 461 – 473.

[10] D. J. Sall, D. L Bailey, J. A. Bastian, J. A. Buben, N. Y. Chirgadze, A. C. Clemens-Smith, M. L. Denney, M. J. Fisher, D. D. Giera, D. S. Gifford-Moore, R. W. Harper, L. M. Johnson, V. J. Klimkowski, T. J. Kohn, H-S. Lin, J. R. McCowan, A. D. Palkowitz, M. E. Richett, G. F. Smith, D. W. Snyder, K. Takeuchi, J. E. Toth, M. M. E. Zhang, J. Med. Chem. 43 (2000) 649 – 663.

[11] G. Phillips, D. D. Davey, K. A. Eagen, S. K. Koovakkat, A. Liang, H. P. Ng, M. Pinkerton, L. Trinh, M. Whitlow, A. M. Beatty, M. M. Morrissey, J. Med. Chem. 42 (1999) 1749-1756.

[12] R. A. Galemmo, Jr., T. P. Maduskuie, C. Dominguez, K. A. Rossi, R. M. Knabb, R. R. Wexler, P. F. W. Stouten, Bioorg. Med. Chem. Lett. 8 (1998) 2705-2710.

[13] T. P. Maduskuie Jr., K. J. McNamara, Y. Ru,R. M. Knabb, P. F. W. Stouten, J. Med. Chem. 41 (1998) 41, 53-62.

[14] K. Sato, T. Kawasaki, Y. Yaniuchi, N. Hismichi, H. Koshio, Y. Matsumoto, Eur. J. Pharmacol**.** 339 (1997) 141-146.

[15] T. Nagahara, Y. Yukoyama, K. Inamura, S. Katakura, H. Yamaguchi, T. Hara, M. Iwamoto, Eur. J. Med. Chem**.** 30 (1995) 139.

[16] T. Nagahara, Y. Yukoyama, K. Inamura, T. Hara, M. Iwamoto, J. Med. Chem. 37 (1994) 1200-1207.

[17] J. Sturzebecher, F. Markwardt, P. Walsmann, Thromb. Res. 17 (1980) 545-548.

[18] J. Sturzebecher, F. Markwardt, P. Walsmann, Thromb. Res. 9 (1976) 637-646.

[19] S. Roehrig, A. Straub, J. Pohlmann, T. Lampe, J. Pernerstorfer, K. Schlemmer, P. Reinemer, E. Perzborn, J. Med. Chem. 48 (2005) 5900 – 5908.

[20] H. Ueno, K. Yokota, J. Hoshi, K. Yasue, M. Hayashi, Y. Hase, I. Uchida, K. Aisaka, S. Katoh, H. Cho, J. Med. Chem. 48 (2005) 3586 – 3604.

[21] M. Nazaré, D. W. Will, H. Matter, H. Schreuder, K. Ritter, M. Urmann, M. Essrich, A. Bauer, M. Wagner, J. Czech, M. Lorenz, V. Laux, V. Wehner, J. Med. Chem. 48 (2005) 4511 – 4525.

[22] S. Maignan, J. Guilloteau, Y. M. Choi-Sledeski, M. R. Becker, W. R. Ewing, H. W. Pauls, A. P. Spada, V. Mikol, J. Med. Chem. 46 (2003) 685 – 690.

[23] D. J. P. Pinto, M. J. Orwat, S. Wang, J. M. Fewig, M. L. Quan, E. Amparo, J. Cacciola, K. A. Rossi, R. S. Alexander, A. M. Smallwood, J. M. Luettgen, L. Liang, B. J. Aungst, M. R. Wright, M. R. Knabb, P. C. Wong, R. R. Wexler, P. Y. S. Lam, J. Med. Chem. 44 (2001) 566-578.

[24] Q. Han, C. Dominguez, P. F. W. Stouten, J. M. Park, D. E. Duffy, R. A. Galemmo Jr., K. A. Rossi, R. S. Alexander, A. M. Smallwood, P. C. Wong, M. M. Wright, J. M. Luettgen, R. M. Knabb, R. R. Wexler, J. Med. Chem. 43 (2000) 4398 – 4415.

[25] Y. K. Yee, A. L. Tebbe, J. H. Linebarger, D. W. Beight, T. J. Craft, D. Gifford-Moore, T. Goodson Jr., D. K. Herron, V. J. Klimkowski, J. A. Kyle, S. Sawyer, G. F. Smith, J. M. Tinsley, R. D. Towner, L. Weir, M. R. Wiley, J. Med. Chem. 43 (2000) 873 – 882.

[26] A. R. Hilgers, R. A. Conradi, S. Burton, Pharm. Res. 7 (1990) 902-910.

[27] L. B. Kier, L. H. Hall, Molecular Connectivity in Chemistry and Drug Research, Academic Press, New York, 1976.

[28] L. B. Kier, L. H. Hall, Molecular Structure Description: the Electro-topological State, Academic Press, New York, 1999.

[29] L. B. Kier, L. H. Hall, in: Devillers J., Balaban, A. T. (Eds.), Topological Indices and Related Descriptors in QSAR and QSPR, Gordon and Breach Science Publishers, Amsterdam, 1999, pp. 455-489.

[30] L. B. Kier, L. H. Hall, Med. Chem. Res. 2 (1992) 497-502.

[31] L. H. Hall, T. A. Vaughn, Med. Chem. Res. 7 (1997) 407-416.

[32] J. Gough, L. H. Hall, J. Chem. Inf. Comput. Sci. 39 (1999) 356-361.

[33] J. Gough, L. H. Hall, Environ. Tox. Chem. 18 (1999) 1069-1075.

[34] L. H. Hall, L. B. Kier, J. Chem. Inf. Comput. Sci. 35 (1995) 1039-1045.

[35] L. B. Kier, L. H. Hall, J. Chem. Inf. Comput. Sci. 40 (2000) 792-795.

[36] K. Rose, L. H. Hall, L. B. Kier, J. Chem. Inf. Comput. Sci. 42 (2002) 651-666.

[37] H. H. Maw, L. H. Hall, J. Chem. Inf. Comput. Sci. 40 (2000) 1270-1275.

[38] H. H. Maw. L. H. Hall, J. Chem. Inf. Comput. Sci. 42 (2002) 290-298.

[39] D. Rogers, A. J. Hopfinger, J. Chem. Inf. Comput. Sci. 34 (1994) 854-866.

[40] L. M. Shi, F. Yi, T. G. Myers, P. M. O'Connor, K. D. Paull, S. H. Friend, J. N. Weinstein, J. Chem. Inf. Comput. Sci. 38 (1998) 189-199.

[41] L. B. Kier, L. H. Hall, J. Mol. Graph. Model. 20 (2001) 76-83.

[42] L. P. Masic, Curr. Med. Chem. 13 (2006) 3627-3648.

[43] M. Ieko, T. Tarumi, T. Nakabayashi, M. Yoshida, S. Naito, T. Koike, Front. Biosci. 11 (2006) 232-248.

Table 1. Factor Xa and thrombin inhibition activity of 3-substituted pyrazole 5-carboxamide analogs.[a]

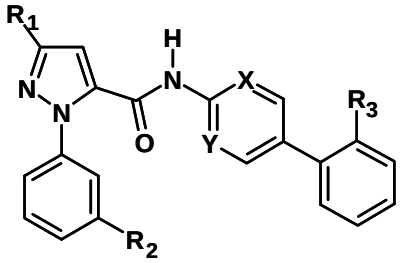

	Substituents				Factor Xa		Thrombin	
	X	*Y*	R_1	R_3	K_I (nM)	pK_I (M)	K_I (nM)	pK_I (M)
Amidine Analogs R_2 = C(NH)NH_2								
Pyr-2a	CH	CH	H	SO_2NH_2	0.16	9.796	900	6.05
Pyr-2b	CH	CH	CH_3	SO_2NH_2	0.013	10.886	300	6.52
Pyr-2c	CH	CH	N-Bu	SO_2NH_2	0.06	10.222	300	6.52
Pyr-2d[b]	CH	CH	CH_3	SO_2NH_2	11	7.959	>2000	---[c]
Pyr-2e	CH	CH	CH_3	SO_2CH_3	0.008	11.097	180	6.74
Pyr-2f	CH	CH	CH_3	CF_3	0.04	10.398	300	6.52
Pyr-2g	CH	CH	CH_3	F	0.46	9.337	450	6.35
Pyr-2h	CH	CH	CH_3	H	1.30	8.886	600	6.22
Pyr-2i	N	CH	CH_3	SO_2NH_2	0.007	11.155	1400	5.85
Pyr-2j	N	N	CH_3	SO_2NH_2	0.041	10.387	7400	5.13
Pyr-2k	C-F	CH	CH_3	SO_2NH_2	0.005	11.301	210	6.68
Pyr-2l	C-Br	CH	CH_3	SO_2NH_2	0.01	11	200	6.70
Pyr-2m	C-Cl	CH	CH_3	SO_2NH_2	0.009	11.046	300	6.52
Pyr-2n	C-F	CH	CH_3	SO_2CH_3	0.02	10.699	230	6.64
Pyr-14a	CH	CH	CF_3	SO_2NH_2	0.015	10.824	40	7.40
Pyr-14b	N	CH	CF_3	SO_2NH_2	0.009	11.046	400	6.40
Pyr-14c	N	N	CF_3	SO_2NH_2	0.01	11	900	6.05
Pyr-14d	C-F	CH	CF_3	SO_2NH_2	<0.005	---[c]	120	6.92
Pyr-14e	CH	CH	CF_3	SO_2CH_3	0.008	11.097	70	7.15
Pyr-14f	C-F	CH	CF_3	SO_2CH_3	<0.005	---[c]	50	7.30
SA862	CH	CH	O (ring)	SO_2NH_2	0.15	9.824	2800	5.55
Benzylamine Analogs R_2 = CH_2NH_2								
Pyr-17a	CH	CH	CH_3	SO_2NH_2	2.70	8.569	21000	4.68
Pyr-17b	C-F	CH	CH_3	SO_2NH_2	1.60	8.796	12000	4.92
Pyr-17c	CH	CH	CH_3	SO_2CH_3	0.89	9.051	21000	4.68
Pyr-17d	C-F	CH	CH_3	SO_2CH_3	0.48	9.319	14000	4.85
Pyr-17e	CH	CH	CF_3	SO_2NH_2	0.91	9.041	14000	4.85
Pyr-17f	C-F	CH	CF_3	SO_2NH_2	0.36	9.444	2000	5.70
Pyr-17g	CH	CH	CF_3	SO_2CH_3	0.38	9.420	5800	5.24
Pyr-17h	C-F	CH	CF_3	SO_2CH_3	0.15	9.824	6000	5.22

[a] Data taken from Pinto et al. J. Med. Chem. 44 (2001) 566 (see ref. 23). [b]This compound has an additional *N*-Me substitution on the pyrazole ring system. [c] Indefinite K_I was not converted to pK_I value.

Table 2. Calculated molecular descriptor values and factor Xa inhibition activity data for subsets of 3-substituted pyrazole 5-carboxamide analogs.

	Substituent	K_I of factor Xa[a]	Molecular Descriptor		
		(pM)[b]	$^3\chi^v_c$	*SHssNH*	*SdNH*
R_1 position					
Pyr-2a	H	160	1.32	2.14	7.60
Pyr-2c	n-Bu	60	1.41	2.15	7.73
Pyr-14a	CF_3	15	1.52	2.25	7.56
Pyr-2b	CH_3	13	1.45	2.14	7.64
R_2 position					
Pyr-17a	CH_2NH_2	2700	1.41	2.13	0
Pyr-2b	$C(NH)NH_2$	13	1.45	2.14	7.64
R_3 position					
Pyr-2h	H	1300	0.77	2.09	7.63
Pyr-2g	F	460	0.82	2.12	7.62
Pyr-2f	CF_3	40	0.97	2.16	7.62
Pyr-2b	SO_2NH_2	13	1.45	2.14	7.64
Pyr-2c	SO_2CH_3	8	1.75	2.14	7.65
R_4 position					
Pyr-2d	CH_3	11000	1.55	0	7.68
Pyr-2b	H	13	1.45	2.14	7.64
X position					
Pyr-2b	CH	13	1.45	2.14	7.64
Pyr-2l	C-Br	10	1.72	2.18	7.66
Pyr-2m	C-Cl	9	1.60	2.20	7.65
Pyr-2i	N	7	1.43	2.20	7.63
Pyr-2k	C-F	5	1.49	2.25	7.62

[a] Taken from Table 1. [b]Presented in picomolar units for easier comparison.

Table 3. Correlation matrix for QSAR model 1 of factor Xa inhibition by pyrazole analogs.

	Activity	$^{3}\chi^{v}_{c}$	***SdssC_acnt***	***SHssNH***
Activity	1.0000	0.2289	0.6074	0.4690
$^{3}\chi^{v}_{c}$		1.0000	-0.3098	0.03234
SdssC_acnt			1.0000	-0.1620
SHssNH				1.0000

Table 4. Inter-model correlation matrix of molecular descriptors used in analysis of factor Xa and thrombin inhibition.

	$^{2}\chi$	$^{3}\chi^{v}_{c}$	***SaaN***	***SdssC_acnt***	***SHdNH***	***SHssNH***
$^{2}\chi$	1.0000	0.6216	0.1498	-0.1135	-0.0995	0.1250
$^{3}\chi^{v}_{c}$		1.0000	-0.0863	-0.3079	-0.3015	0.0313
SaaN			1.0000	0.1705	0.1780	0.0903
SdssC_acnt				1.0000	0.9998[a]	-0.1569
SHdNH					1.0000	-0.1530
SHssNH						1.0000

[a]The nearly 100% inter-correlation is justified by the fact that the two molecular descriptors are representing the different atom types in the same functional group (imine), *SHdNH* represents the H of imino nitrogen, while *SdssC_ant* represents the carbonyl carbon of imine.

Table 5. Caco-2 cell permeabilities of 3-substituted pyrazole 5-carboxamide analogs.[a]

	Substituents				Cell Permeability
	X	*Y*	R_1	R_3	pK_P (μM)
Amidine Analogs R_2 = $C(NH)NH_2$					
Pyr-14c-17	N	N	CF_3	SO_2NH_2	7.0
Pyr-14f-20	CF	CH	CF_3	SO_2CH_3	6.7
Benzylamine Analogs R_2 = CH_2NH_2					
Pyr-17a-21	CH	CH	CH_3	SO_2NH_2	6.7
Pyr-17b-22	CF	CH	CH_3	SO_2NH_2	6.0
Pyr-17c-23	CH	CH	CH_3	SO_2CH_3	5.9
Pyr-17d-24	CF	CH	CH_3	SO_2CH_3	5.5
Pyr-17f-26	CF	CH	CF_3	SO_2NH_2	6.0
Pyr-17g-27	CH	CH	CF_3	SO_2CH_3	5.5
Pyr-17h-28	CF	CH	CF_3	SO_2CH_3	5.3

[a] Data taken from Pinto et al. J. Med. Chem. 44 (2001) 566 (see ref. 23).

Figure Legends

Figure 1. Structure of pyrazole carboxamides investigated for QSAR studies. Substituents varied were located at the R_1, R_2, R_3, R_4 and X positions.

Figure 2. Predictive ability of a QSAR model (Model 1) for factor Xa inhibition by 3-substituted pyrazole 5-carboxamide analogs.

Figure 3. Predictive ability of a QSAR model (Model 3) for thrombin inhibition by 3-substituted pyrazole 5-carboxamide analogs.

Figure 4. Predictive ability of a QSAR model (Model 4) for Caco-2 cell permeability of high-affinity 3-substituted pyrazole 5-carboxamide derivatives.

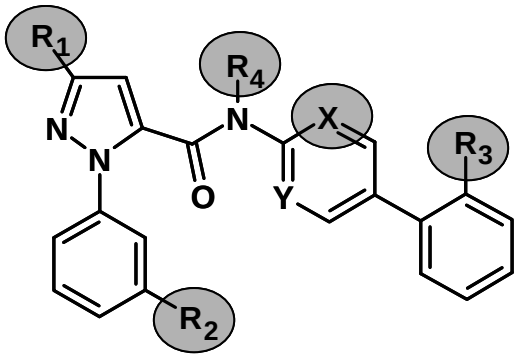

Figure 1

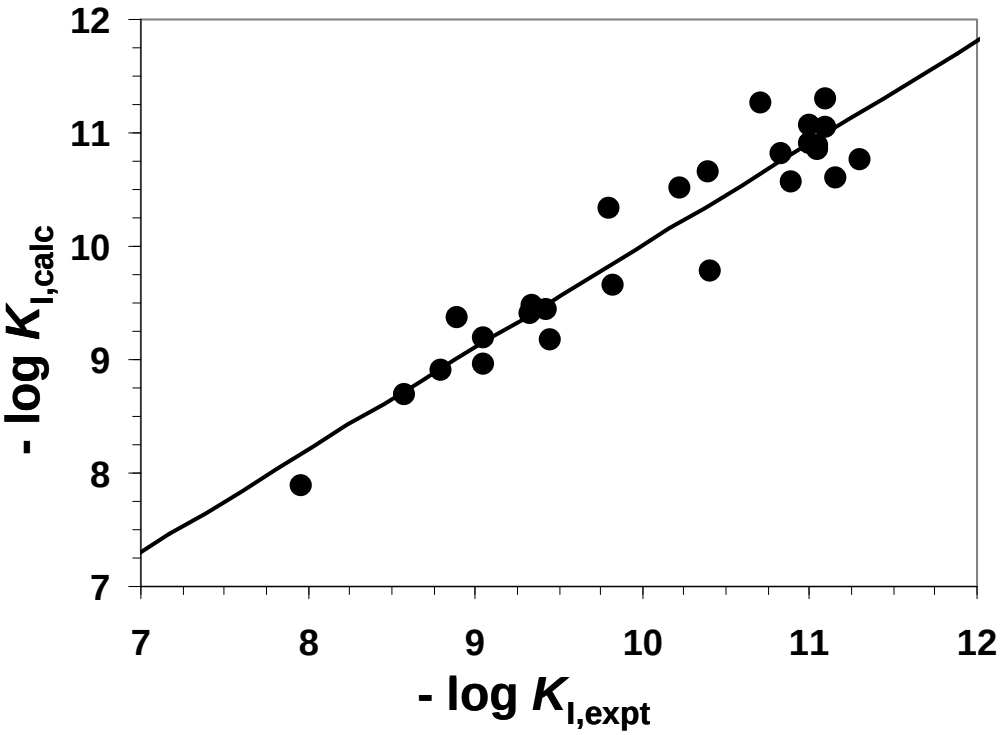

Figure 2

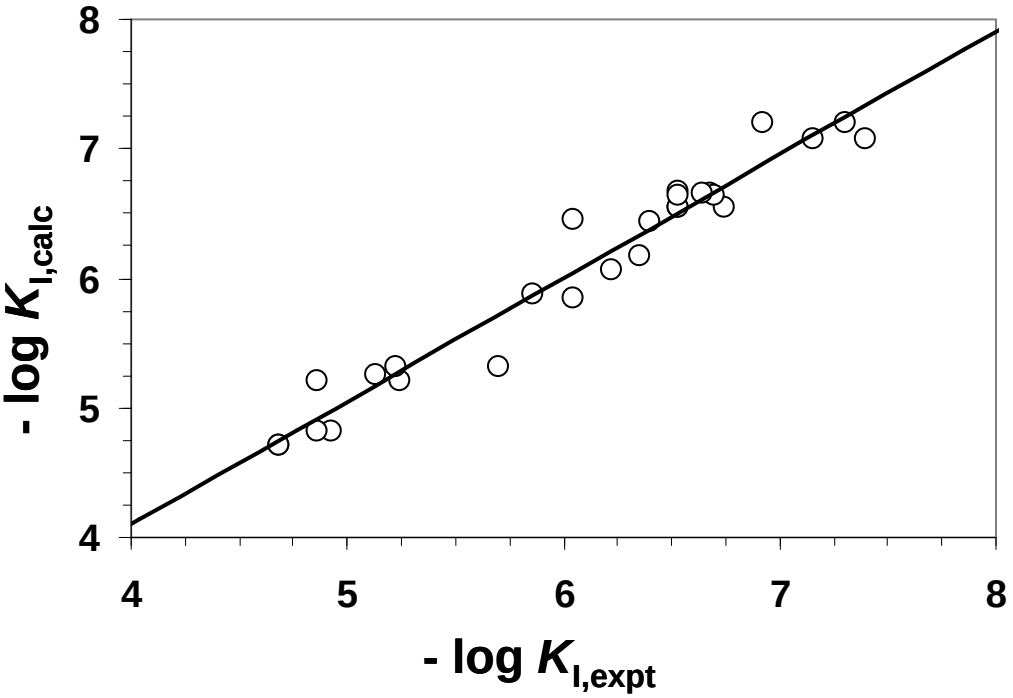

Figure 3

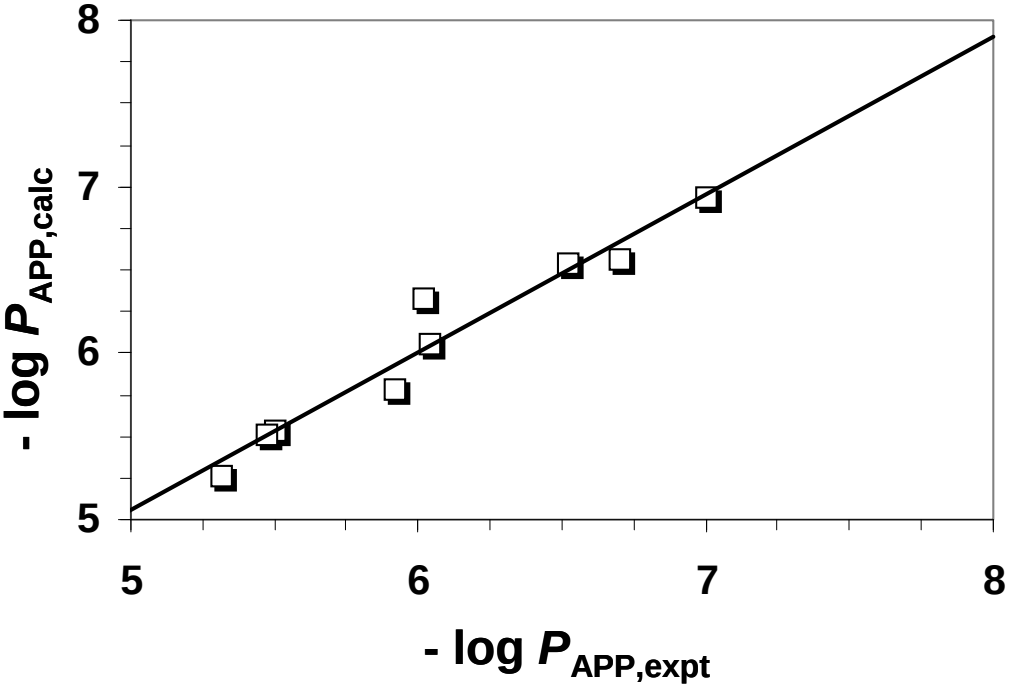

Figure 4